Capillary rise quantifications based on in-situ artificial deuterium peak displacement and laboratory soil characterization

Olivier Grünberger, J.L. Michelot, L. Bouchaou, P. Macaigne, Y. Hsissou, C. Hammecker

▶ **To cite this version:**

Olivier Grünberger, J.L. Michelot, L. Bouchaou, P. Macaigne, Y. Hsissou, et al.. Capillary rise quantifications based on in-situ artificial deuterium peak displacement and laboratory soil characterization. Hydrology and Earth System Sciences, 2011, 15 (5), pp.1629-1639. 10.5194/hess-15-1629-2011 . hal-02644454

HAL Id: hal-02644454
https://hal.inrae.fr/hal-02644454v1

Submitted on 28 May 2020

HAL is a multi-disciplinary open access archive for the deposit and dissemination of scientific research documents, whether they are published or not. The documents may come from teaching and research institutions in France or abroad, or from public or private research centers.

L'archive ouverte pluridisciplinaire **HAL**, est destinée au dépôt et à la diffusion de documents scientifiques de niveau recherche, publiés ou non, émanant des établissements d'enseignement et de recherche français ou étrangers, des laboratoires publics ou privés.

Hydrol. Earth Syst. Sci., 15, 1629–1639, 2011
www.hydrol-earth-syst-sci.net/15/1629/2011/
doi:10.5194/hess-15-1629-2011
© Author(s) 2011. CC Attribution 3.0 License.

Hydrology and Earth System Sciences

Capillary rise quantifications based on in-situ artificial deuterium peak displacement and laboratory soil characterization

O. Grünberger[1], **J. L. Michelot**[2], **L. Bouchaou**[3], **P. Macaigne**[4], **Y. Hsissou**[3], **and C. Hammecker**[5]

[1]Institut de Recherches pour le Développement, UMR Lisah, Campus SupAgro, Montpellier, France
[2]Université Paris-Sud, CNRS, UMR IDES, Orsay, France
[3]Université Ibn Zohr, Laboratoire de Géologie Appliquée et Géo-Environnement (LAGAGE), Agadir, Morocco
[4]Université Paris-Sud, Dép. Sciences de la Terre, Orsay, France
[5]Institut de Recherches pour le Développement, UMR Eco & Sol, Campus SupAgro, Montpellier, France

Received: 19 August 2010 – Published in Hydrol. Earth Syst. Sci. Discuss.: 5 October 2010
Revised: 21 April 2011 – Accepted: 9 May 2011 – Published: 27 May 2011

Abstract. In arid environments, water rises from the saturated level of a shallow aquifer to the drying soil surface where evaporation occurs. This process plays important roles in terms of plant survival, salt balance and aquifer budget. A new field quantification method of this capillary rise flow is proposed using micro-injections (6 µL) of a deuterium-enriched solution (δ value of 63 000‰ vs. V-SMOW) into unsaturated soil at a 1 m depth. Evaluation of peak displacement from profile sampling 35 days later delivered an estimate that was compared with outputs of numerical simulation based on laboratory hydrodynamic measurements assuming a steady state regime. A rate of 3.7 cm y^{-1} was estimated at a Moroccan site, where the aquifer water depth was 2.44 m. This value was higher than that computed from the relationship between evaporation rates and water level depth based on natural isotopic profile estimates, but it was lower than every estimate established using integration of the van Genuchten closed-form functions for soil hydraulic conductivity and retention curve.

1 Introduction

In arid environments with long periods of high evaporative demand, water may rise from the saturated level of a shallow aquifer to the near surface of the drying soil where evaporation occurs. Although resulting evaporation rate is known to decrease quickly with aquifer depth, this process may play important roles in terms of plant survival, salt balance and aquifer budget. Field quantification of capillary rise in soil is difficult to perform. First, the stability of water contents along the soil profile does not allow the closure of traditional soil budget to be performed by using time differences in soil water stocks. Second, the low suction values in soil (lower than -800 cm) that are frequently encountered near the soil surface outrange tensiometer measurement capability. Fluxes smaller than 100 mm y^{-1} are not easily measured, other than by external surface measurements such as the eddy-covariance method (Garcia et al., 2009). Significant advances were achieved in the early eighties with a method that was developed to compute steady-state evaporation rates using equilibrium between convection and diffusion of natural stable isotopic species (^{2}H, ^{18}0) in the liquid and vapor phases of vadose zone profiles under arid conditions (Allison, 1982; Barnes and Allison, 1983, 1984; Barnes and Hughes, 1983; Fontes et al., 1986). Initially conceived for very arid conditions, this method was progressively extended to semi-arid conditions with shorter profiles, where a "pseudo steady-stage of evaporation" was considered to be reached at the end of the dry season (Liu B et al., 1995; Yamanaka and Yonetani, 1999; Grünberger et al., 2008). Additionally, modeling was refined by taking into account dynamics of drying processes and interactions with plant evapotranspiration (Walker et al., 1988; Barnes and Walker, 1989; Shimojima et al., 1990; Walker and Brunel, 1990; Brunel et al., 1995, 1997; Melayah and Bruckler, 1996a, b; Braud et al., 2005a, b). The profiles of isotope contents allowed discrimination between the top layer, where only vapor fluxes occur, and the deeper layers, where liquid-phase fluxes are dominant. A better understanding of the partition processes

Correspondence to: O. Grünberger
(olivier.grunberger@ird.fr)

between water and vapor fluxes was the main outcome provided by these studies, but some uncertainties remain concerning field flux measurements. Because soil profile sampling cannot be repeated in the same place, the calculated evaporation rates are "instant rates", subjected to night and day alternation and temperature fluctuation, which may differ from the time average value. Gardner (1958) was the first author to propose a relationship based on a specific integration of the Richards equation to determine rise rate by capillarity assuming a steady state of the soil profile. This relationship linked the depth of the saturated level, the soil hydrodynamic characteristics and an ascending rate assumed to be constant along the whole profile. It was confirmed by measurements on experimental columns of disturbed or undisturbed soils submitted to capillary rise under different conditions (Gardner and Fireman, 1958). Although vapor fluxes were not considered separately from liquid fluxes and the expression could not account for layered soils, this method has been widely used to compute the relation between the depth of the water table and the stabilized evaporation flux. A comparison between flux estimates based on the Gardner approach and flux estimates obtained from isotopic profiles was performed by Coudrain-Ribstein et al. (1998). The rates computed with natural isotopic profiles collected in this latter study led to an average relationship between evaporation (E in $\mathrm{mm\,y^{-1}}$) and depth of the aquifer (z in meters): $E = 71,9\ z^{-1.49}$. Applying the Gardner equation and taking into account sufficient ranges of permeability and suction for sandy and loamy soils resulted in a rate interval of $[28\,z^{-1,8},\ 205\,z^{-1,6}]$. The introduction of the van Genuchten (1980) "closed-form equation" to represent soil permeability was used by Hu et al. (2008) to perform a theoretical analysis of the steady-state rate of capillary rise by evaporation.

Putting apart the profiles of natural isotope contents in soil water already evocated, many studies considered the use of artificial isotopic species of water as tracers in soil hydrodynamic studies (Koeniger et al., 2010). However, field and laboratory soil hydrodynamic studies involving isotopic tracers mainly focused on infiltration and/or mixing fronts and implied large volumes of tracing solution resulting in almost (or totally) saturated conditions. To our knowledge, artificial tracing has never been used to quantify field capillary rise. Recently, Garcia et al. (2009) studied the tritium release from the vadose zone to the atmosphere near a low-level radioactive waste facility in the southern Nevada desert, but tritium fluxes were only calculated as simple products of evapotranspiration fluxes (measured by the eddy covariance method) and tritium concentrations in water vapor.

Our objectives were to assess a new method of field measurement of capillary rise flow and to bring out a foundation of comparison with the results of simulation based on laboratory hydrodynamic measurements. We based our approach on the practices of eco-physiologists who perform small volume injection of a concentrated solution to quantify tree sapflow (Marc and Robinson, 2004). A small quantity of artificial D_2O was injected into a soil profile, and the displacement of the tracer was measured 35 days later. The site and injection time were selected to present characteristics favorable to approach nearly steady-state drying conditions, to allow comparison of the rate computed from the tracer peak displacement to the rates based on laboratory soil measurements and simulations assuming a steady-state regime in relation to specific field boundary conditions.

2 Materials and methods

2.1 Site description

The experiment site is located at 30°22′05 N 09°34′38 W near Agadir city, Morocco. The experiment was performed in 2001 on a sandy soil with a shallow free aquifer (Bouchaou et al., 2008) approximately 2.6 km from the coast. The soil consists of a fine eolian sand cover with a modal size of approximately 100 µm and moderate carbonate contents (Weisrock et al., 2002). The nearest meteorological station is located 14 km away from the sampling site at Agadir International Airport. At this station, the annual rainfall was exceptionally low in 2001 (year of the experiment), with a value of 86 mm, whereas the average annual rainfall recorded between 1961 and 2004 was $255\,\mathrm{mm\,y^{-1}}$ (Stour and Agoumi, 2008). The experiment started on 16 May 2001 and ended on 20 June 2001; it was carried out at the end of a pronounced drought period of 5 months. Since the beginning of 2001, a total precipitation of 12 mm was confronted with a high evaporative demand, characterized by an annual potential evaporation higher than $2000\,\mathrm{mm\,y^{-1}}$ (Bouchaou et al., 2008). The daily precipitation, recorded at the station since the beginning of 2001, never exceeded 4 mm. These recorded amounts were 0.7 mm 25 days before the experiment, 0.51 mm 70 days before the experiment, and 3.05 mm 75 days before the experiment. Before excavating the experimental pit, a 3-m-deep hole was drilled with a helical hand auger. The hole allowed us to check that the aquifer water level was about 2.5 m deep and that the fine eolian sand cover was thicker than 3 m at the selected site. A shallow free aquifer in sandy material was a requirement for this experiment. A well-piezometer for measuring the free water table level was created by inserting a 3 m-long, 2 inch-diameter PVC tube, screened on 2 m length into the auger hole to set the first 50 cm of the screen under the water level. Water level measurements were performed using an electric flat tape water level meter. Values were corrected in reference to the ground level. The depth of the water level was measured one hour after the setting of the tube, one day after filling the injection pit and just before and after sampling the tracer (35 days later). All measurements delivered the same value (2.44 m). Relative humidity was monitored with a moisture capacity probe at the soil surface and at five depths (7 cm, 10 cm, 19 cm, 23 cm and 31 cm) in the profile during the sampling

Table 1. Relative humidity (%) measured on 19, 20, 21 and 22 June 2001 in the soil top layer aside the sampling pit. For a 0 cm depth measurement, the capacitance probe was at the soil surface. For 7 cm, 10 cm, 20 cm, 23 cm and 31 cm depths, the probe was inserted in a 40-cm long PVC tube driven horizontally in the soil from the wall of a pit. Measurements were taken after 5 min contact with soil moisture. (Avg. = average, [Min-Max] = interval of extreme values, Nb = Number of measurements, σ = Standard deviation).

	Late Night (02:00–06:00 h)				Midday (10:00–14:00 h)				Early night (22:00–02:00 h)			
Depths	Avg.	[Min–Max]	Nb	σ	Avg.	[Min–Max]	Nb	σ	Avg.	[Min–Max]	Nb	σ
0 cm	81.8	[81.6–82.6]	6	0.6	47.1	[31.0–62.6]	8	9.8	75.2	[73.4–78.7]	5	2.1
7 cm	77.1	[76.5–78.0]	6	0.5	57.0	[50.0–64.6]	8	4.9	73.6	[70.3–77.5]	5	3.0
10 cm	81.0	[79.7–81.6]	5	0.7	66.4	[62.7–70.2]	7	2.5	78.8	[77.2–81.4]	5	1.8
19 cm	82.1	[81.8–82.4]	5	0.2	73.6	[69.1–77.8]	7	3.3	79.4	[78.4–81.6]	6	1.3
23 cm	86.7	[85.8–88.2]	5	1.0	79.9	[76.5–84.5]	7	3.0	84,1	[83.3–85.6]	6	0.8
31 cm	87.8	[87.2–88.9]	5	0.7	84.7	[80.2–88.4]	7	2.9	84.9	[83.6–86.4]	6	1.2

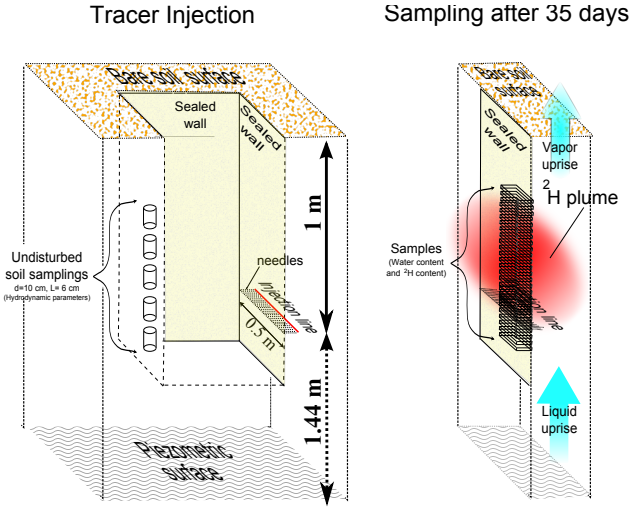

Fig. 1. Block diagram presenting injection pit and recovering sampling procedures of D tracer in the soil profile.

day and the three following days (Table 1). The values at the soil surface ranged from 31.0% at midday to 82.6% early in the morning, but they were always higher than 80.2% at 31 cm depth.

2.2 Deuterium injection, sampling and measurements

On 16 May 2001, a squared pit was excavated to a depth of more than 1 meter. Sampling to determine laboratory soil hydrodynamic parameters (Fig. 1) included 5 undisturbed core samples (diameter 10 cm and length 8 cm). Five cylinders of 98 cm^3 were also collected from 3 cm to 114 cm for water content measurements (Fig. 2). An horizontal injection line was settled at a depth of 1 m on the wall of the pit (Fig. 1). This depth was chosen assuming that transfer in vapor phase was not dominant and negative potential heads were not higher than −800 cm at a depth between 50 cm and 100 cm in the soil layer. Fifty injection points were defined by driving 47-mm-long medical needles, spaced 1 cm apart, in the soil along a horizontal line on a side of the pit at 100 cm depth. The thin needle of a 10 µL micro syringe was inserted inside the medical needles, which acted as a catheter, to inject 6 µL of deuterium-enriched solution. This artificial solution was prepared by mixing a small amount of heavy water D_2O (99.9 %) with laboratory deionized water, resulting in a $R_{D/H}$ of 0.009968 (corresponding to a δ value of 63000 δ ‰ vs. V-SMOW). The total input corresponded to 1.67×10^{-4} moles of D_2O. Immediately after excavation, spray-paint was used to seal the pit wall surface to prevent drying during the injection time (1.5 h for the 50 points), mitigate the effects of the disturbance due to the pit, and ease the correct placement of the sampling as a land mark. After the injection, the medical needles were left in the soil, and the pit was filled up respecting the sequence of the extracted soil. Thirty-five days later, soil sampling was performed above the injection line to retrieve the tracer along a column (Fig. 1) adjacent to the spray-paint coating. Soil was progressively removed horizontally, slide by slide, following the spray-paint coating that was used as a landmark, with a rectangular (15 cm x 5 cm) steel frame. For each sampling, the frame was oriented with the 15-cm-long side beside the paint coating line, in a horizontal position and centered upon the 50 cm injection line. After measurement of the sampling depth, the frame was driven 0.5 cm inside the upper part of the soil column. Only the soil inside the frame was sampled.

Water extraction and deuterium analysis were performed on 17 samples taken between 113 cm and 43 cm depths. The Deuterium concentrations were determined after reduction of the distilled water by reaction with zinc (Coleman et al., 1982) using a mass spectrometer VG602C. The results are reported in δ-notation, permil deviation of the measured isotopic ratio relative to V-SMOW international standard, with an uncertainty less than $\pm 2\delta$‰. The tracer injection produced a sharp peak of deuterium content in the soil profile. The peak displacement with time may be interpreted as the

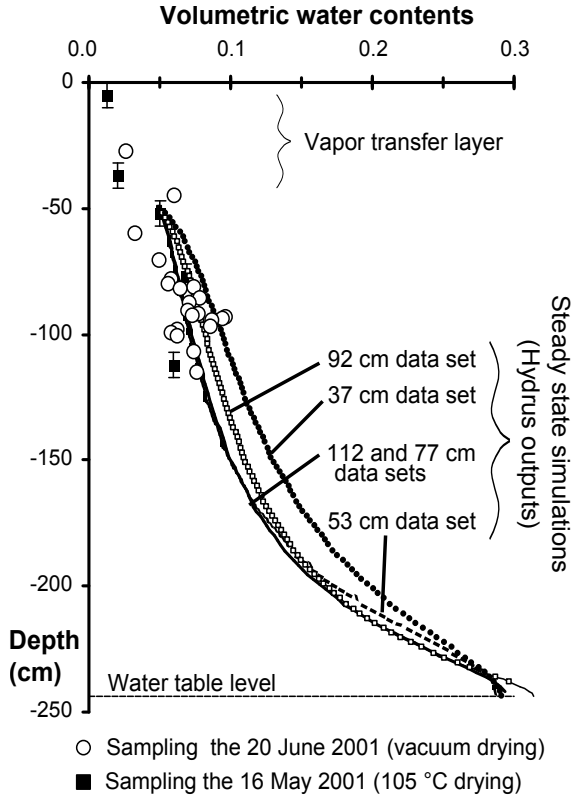

Fig. 2. Soil volumetric water contents in the sampled pit, on 16 May 2001 and 20 June 2001. Steady state Hydrus 1D water content profiles with the five different sets of van Genuchten hydrodynamic parameters. Because water contents were very low in the upper part of the profile (depths <50 cm), significant vapor transfer was suspected. Consequently, the top layer of the profile was not considered in the simulation. Estimated accuracy was 0.5 cm in level and 0.5% in water content.

result of the cumulative convective upward flow. When no evaporation or preferential fluxes takes place, the amount of water between the injection depth and the final peak depth represents the volume of displaced water during the period between injection and sampling:

$$E_{35\ \mathrm{days}} = \int_{\mathrm{inj}}^{\mathrm{peak}} \Theta(z) \cdot dz \tag{1}$$

where $E_{35\ \mathrm{days}}$ is the water flux during the 35 days (cm) at the injection depth, inj is the injection depth (cm), peak is the peak depth (cm), and $\Theta(z)$ is the measured volumetric water content 35 days after the injection at the depth z.

2.3 Soil parameters and rise rate computation

Soil hydrodynamic parameters were characterized using the evaporation method and five undisturbed samples taken on one side of the pit (Wind, 1968). The software Hydrus 1D.4.13 was used to calculate values of the van Genuchten (1980) hydrodynamic parameter by inversion (Simunek et al., 1998). The inversions were based on selected data extracted from the laboratory drying curves of saturated undisturbed soil samples. Eight pairs of data consisting of times and tension heads and pairs of times and water content data were selected. The initial values of the van Genuchten parameters were approximated by the direct method in a spread sheet file, and consistency was checked. Saturated water content (Θ_s) was not included in the set of parameters to adjust with the inversion process and was kept unchanged from the laboratory measurement. Results are presented in Table 2. We respected the van Genuchten (1980) formalism, where S is the saturation index, Θ_r and Θ_s are the residual and saturation contents, respectively, ψ is the tension head [L], K(ψ) is the hydraulic conductivity [L T^{-1}] and Ks is the saturated hydraulic conductivity [L T^{-1}], α ([L^{-1}],cm^{-1}), n, m=1-1/n are the other van Genuchten parameters using the following relations:

$$S = \frac{\Theta - \Theta_r}{\Theta_s - \Theta_r} = (1 + (\alpha\psi)_n)^{-m} \tag{2}$$

$$K(\psi) = K_s S^{1/2} (1 - (1 - S^{1/m})^m)^2 \tag{3}$$

The vertical flux is described by the Richards differential equation linking the flux E ([L T^{-1}], cm min^{-1}) and the hydraulic conductivity ([L T^{-1}], cm min^{-1}) to the variation of the potential head ψ [L], cm along the depth Z ([L], cm$^{-1.}$), Z=0 at the soil surface and Z>0 inside the soil:

$$E = K(\psi) \cdot \frac{d\psi}{dz} - K(\psi) \Leftrightarrow dz = \frac{K(\psi)}{E + K(\psi)} d\psi \tag{4}$$

At a steady state, between two depths z_1 and z_2 ([L], cm), stabilized at the constant potential heads ψ_1 and ψ_2 ([L], cm), the flux E is constant and ruled by the integration of Eq. (4):

$$\int_{z1}^{z2} dz = \int_{\psi 1}^{\psi 2} \frac{K(\psi)}{E + K(\psi)} d\psi = z_2 - z_1 \tag{5}$$

In a steady-state evaporation profile, when the soil characteristic relationships $K(\psi)$ and $\psi(\theta)$ are known, then the vertical convective flux (E) between these two points can be computed. A particular starting point of integration may be the groundwater level, where soil saturation implies that the tension head is equal to zero (then z_1=0 and ψ_1=0). A potential maximum evaporation flux may be computed by setting z_2 to the depth of the groundwater level and ψ_2 to ∞. Assuming a steady state condition, Eq. (5) may be applied using particular field-measured water contents at known depths as boundary conditions. Equation (5) was solved numerically by Eq. (6) developed in a spreadsheet using 36 600 integration steps:

$$z_2 - z_1 \approx \sum_{i=0}^{i=36660} \frac{K(\psi(i))}{E + K(\psi(i))} \Delta\psi(i) \tag{6}$$

Table 2. Van Genuchten hydrodynamic parameter measurements for five undisturbed soil samples. Measurements were performed using Wind methods with parameter adjustment by inversion using the Hydrus (1.4) software. The resulting potential head (ψ) for a water content of 0.0495. (in bold: geometric mean).

Sampling depths	Θ_r	Θ_s	α	n	K_s	$\psi(0.0495)$
cm	–	–	cm^{-1}	–	$cm\,min^{-1}$	cm
37	0.012	0.291	0.0289	1.7770	0.2478	−455.3
53	0.030	0.287	0.0304	2.2067	0.6615	−277.6
77	0.008	0.314	0.0565	1.6320	0.6045	−416.2
92	0.014	0.295	0.0413	1.8360	0.5996	−285.9
112	0.014	0.310	0.0378	1.9157	0.3639	−266.5
Average	0.0156	0.2994	0.0390	1.8735	**0.4645**	−340.3

Table 3. Steady state fluxes (cm) for 35 days, computed using Eqs. (5) and (3) with three different sets of boundary conditions and five soil data sets (Table 2). (in bold: geometric mean). Z_1 is the depth of upper limit (cm), Z_2 the depth of lower limit (cm). Θ_1 and Θ_2 are the water contents at depths Z_1 and Z_2. Θ_s is the saturated water content, and $\psi(\Theta_1)$, the potential head (cm) at the depth Z_1. Sets *i*, *ii* and *iii* correspond to integration boundaries representative of field measurements.

Van Genuchten Data sets	Boundary sets	*i*	*ii*	*iii*
	Upper boundary	$\psi(\Theta_1) = -1.64\times10^6$ cm $Z_1 = 0$ (soil surface)	$\Theta_1 = 0.0495$ $Z_1 = 50$ cm	$\Theta_1 = 0.03546$ $Z_1 = 37$ cm
	Lower boundary	$\Theta_2 = \Theta_s$ $Z_2 = 244$ cm	$\Theta_2 = \Theta_s$ $Z_2 = 244$ cm	$\Theta_2 = 0.07623$ $Z_2 = 100$ cm
37 cm		1.56	3.46	1.17
53 cm		0.58	1.41	1.82
77 cm		0.59	1.09	0.75
92 cm		0.72	1.33	1.60
112 cm		1.20	0.77	1.03
Geometric mean		**0.86**	**1.40**	**1.21**

using Eqs. (2) and (3) and with:

$$\psi(i+1)=\psi(i)+\Delta\psi(i) \quad (7)$$

computing proportional integration steps:

$$\Delta\psi(i)=\lambda\psi(i) \quad (8)$$

or using a constant for the integration steps:

$$\Delta\psi(i)=\gamma \quad (9)$$

Uprising fluxes were estimated for each set of unsaturated soil characteristics established by the Wind's method using three distinct sets of integration limits and results are summarized in Table 3.

The first integration (*i*) was computed between the aquifer level (saturation depth) at a depth of 244 cm, where $\psi(0) = 0.0001$ and the soil surface with a maximum tension head of $\psi(i = 36\,600)$=-1.6410^6 cm, and corresponding to the minimum relative air humidity of 31% observed at the soil surface. The parameter λ was set to 1.000624294 (Eq. 8).

The second integration (*ii*) was calculated between the saturation depth at 244 cm, where $\psi(0)$=0.0001 cm, and at the 50 cm depth, where water content was set to the field-measured value (1). The parameter λ was set so as to reach this value for the same number of integration steps (Eq. 8).

The third integration (*iii*) considered the lower limit at 100 cm depth, where water content was set to 0.076227. The upper limit was set to a depth of 37 cm, where water content was 0.03546 to mimic the trend of average water content increase. Due to the smaller gap of tension heads, the constant γ was set so as to reach the same number of integration steps (Eq. 9).

The results of the integration methods *ii* and *iii* were compared to a numerical simulation computed with Hydrus1D4.13 and using the same parameter set and boundary conditions (Table 4). The initial condition for water content was settled to an increasing linear trend with depth from a water content of 0.1 at the surface to saturation at 244 cm depth. Total run time was set to 100 days, and stability of fluxes and water content was always observed after 20 days.

The value reported in Table 4 is the value of "surface flux" for 100 days.

3 Results

3.1 Soil water contents and van Genuchten parameters

The profile of the soil volumetric water content is presented in Fig. 2. The soil water content between the surface and 120 cm depth was always lower than 0.097. The water content was inferior to 0.026 between the surface and the 40-cm depth. A linearly increasing trend in soil water content with depth was observed, with a low correlation ($R^2 = 0.66$) and a slope of 6.64 10^{-4} (θ cm^{-1}). This correlation was stronger ($R^2 = 0.84$) between depths of 60 cm and 97 cm with a slope of 1.543×10^{-3} (θ cm^{-1}). The distribution of the water content values with depth indicates that the retention parameters were quite heterogeneous throughout the soil at the small scale. The saturation water content was quite constant along the soil profile, ranging from 0.29 to 0.31 (Table 1). The parameter n, ranging from 1.6 to 2.2, is representative of sandy loam, loamy sands and loams, and the parameter α, ranging from 0.029 cm^{-1} to 0.056 cm^{-1}, typically corresponds to loams and sandy loams. The measured saturated hydraulic conductivity ranged from 0.25 cm min^{-1} to 0.66 cm min^{-1}, which are values associated with fine sands and loamy sands, respectively. The small size of the sand particles (100 µm) (Weisrock et al., 2002) may explain the high hydraulic conductivity values combined with low α values. The application of Eq. (2) shows that the tension heads that correspond to water content of 0.0495 (the value at 50 cm depth) range from −455 cm to −266 cm and they fall into two groups of similar values. The first group corresponds to sampling characterization depths of 37 cm and 77 cm and the second one to the samplings at depths of 53 cm, 92 cm and 112 cm.

3.2 Fluxes estimated using soil laboratory characterization

The computed vertical fluxes for 35 days while assuming steady-state evaporation are reported in Table 3. The cumulative fluxes range from 0.59 cm to 3.46 cm for the 35 days (corresponding to 61 mm y^{-1} to 390 mm y^{-1}). The geometric mean is an appropriate averaging value in a soil profile with layered hydraulic conductivity; it provides an indicator of the overall capability of vertical transfer. The geometric mean hydraulic conductivity is also appropriate in the case of an assumed statistical log-normal distribution, which is frequently encountered in experimental soil data (Jim Yeh and Harvey, 1990). The geometric means of estimates using integrations based on Eq. (5) with *i*, *ii* and *iii* sets of limits (Table 3) ranged between 0.86 cm and 1.40 cm for 35 days (corresponding to 89 mm y^{-1} to 146 mm y^{-1}), with an overall arithmetic average of 1.27 cm for the 35 days (corresponding to 133 mm y^{-1}). The comparison of the results

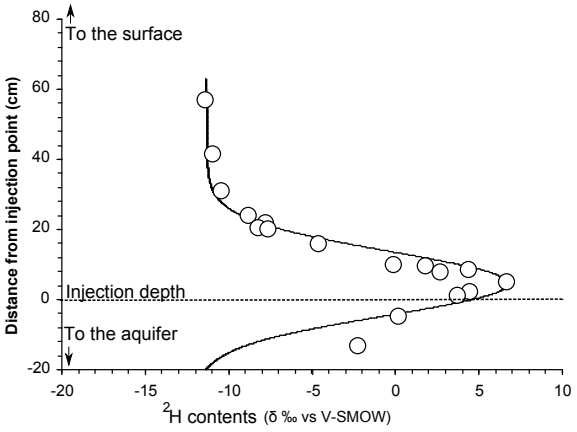

Fig. 3. Deuterium contents (δ ‰ vs. V-SMOW) of soil water in function of the distance to the injection point 35 days after tracer injection. The curve corresponds to the best Hydrus 2D fit with steady-state water regime assumption with the soil parameters. ($\Theta_r = 0.0304$, Θ_s, $= 0.287$, $\alpha = 0.0304$ cm^{-1}, $K_s = 0.22$ cm min^{-1}, $n = 2.207$ and a longitudinal dispersivity = 8.15 cm and Lateral dispersivity = 2.24 cm).

obtained by methods *ii* and *iii* (Table 3) with the Hydrus run estimates (Table 4) shows that although the order of magnitude of fluxes is similar in all situations but one (37 cm depth, method *iii*), the Hydrus1D estimates are higher than those computed directly by the integration function. The differences between geometric means were less than 10% using the two methods and the boundary conditions *ii* and *iii*. The maximum obtained difference between methods for a particular data set is 18% (data set 53 cm, *ii*). The influence of an error on the field-measured volumetric water content and of a change of water level depth on the Hydrus simulation estimates was tested (Table 4). An increase of 1% in water content at 50 cm (i.e., 0.0595 instead of 0.0495) led to a decrease in fluxes by 13% (37 cm) to 83% (112 cm). A decrease of 1% resulted in a rate increase ranging from 6% (37 cm) to 37% (112 cm). Similarly, a 10-cm increase in depth water level (i.e., 2.54 m instead of 2.44 m) led to a rate decrease of 18% (77 cm) to 27% (53 cm). A free aquifer level located 10 cm higher (2.34 m depth) resulted in rates increased by 21% (37 cm) to 36% (53 cm).

3.3 Injection results

A sharp peak of high ^{2}H concentrations was observed in soil water (Fig. 3). The maximum δ ^{2}H content was +6.7‰ vs. V-SMOW at a distance of 4.7 cm from the injection point. The δ^2H value was −11.7‰ vs. V-SMOW at a distance of 56.8 cm (44.2 cm depth). Positive δ values were recorded at distances between +9.5 cm and –5 cm from the injection point. The average soil water content between depths of 100 cm and 95.3 cm was 0.0747. A 47-mm displacement corresponded to a flux of 0.351 cm in 35 days, or 3.66 cm y^{-1}

Table 4. The steady state capillary rise rate (cm) for 35 days based on Hydrus simulations for five van Genuchten data sets (Table 2) and six sets of boundary conditions. Boundary conditions sets *ii* and *iii* are similar to Table 3. (In bold: geometric mean). Z_1 is the depth of upper limit (cm), Z_2 the depth of lower limit (cm). Θ_1 and Θ_2 are the water contents at depths Z_1 and Z_2. Θ_s is the saturated water content. Boundary conditions sets *ii* and *iii* correspond to field measured conditions.

		Boundary conditions sets *ii* and *iii*		Aquifer level depth change		Upper water content change	
	Upper boundary	Θ_1=0.0495 Z_1 = 50 cm	Θ_1=0.0346 Z_1 = 37 cm	Θ_1=0.0495 Z_1 = 50 cm	Θ_1=0.0495 Z_1 = 50 cm	Θ_1=0.0595 Z_1 = 50 cm	Θ_1=0.0395 Z_1 = 50 cm
van Genuchten Data sets (Table 2)	Lower Boundary	$\Theta_2=\Theta_s$ Z_2 = 244 cm	Θ_2=0.07623 Z_2=100 cm	$\Theta_2=\Theta_s$ Z_2=254 cm	$\Theta_2=\Theta_s$ Z_2=234 cm	$\Theta_2=\Theta_s$ Z_2 = 244 cm	$\Theta_2=\Theta_s$ Z_2 = 244 cm
37 cm		3.74	1.13	2.99	4.52	3.27	3.98
53 cm		1.62	2.15	1.19	2.21	0.17	2.04
77 cm		1.26	0.79	1.03	1.54	0.99	1.39
92 cm		1.34	1.87	1.02	1.75	0.42	1.74
112 cm		0.83	1.14	0.62	1.12	0.14	1.14
Geometric mean		**1.53**	**1.33**	**1.18**	**1.98**	**0.50**	**1.86**

(Eq. 1). The values computed using Eq. (5) with a steady-state assumption and based on laboratory measurements (Table 3) are 1.66 to 9.86 times higher than the rate computed from the peak displacement. Tracer recovering was computed by peak integration. The barycentre of ^{2}H concentrations weighted by water contents was determined using an initial δ^2H content of -11.7 ‰ vs. V-SMOW and indicated an average distance of 2.4 cm. This result must be mitigated due to the fact that only a few measurement points were performed under the injection point because a preliminary assumption was that the convective flux would be higher. Because sampling was performed on a determined surface imposed by the sampling steel frame, a recovery rate of the tracer can be estimated. After 4.698×10^{-5} moles of D_2O were injected into the soil column (on 15 cm of the line of injection), 2.29×10^{-5} moles were recovered in the 15 cm × 5 cm sampling area, and this corresponds to a recovery rate of 48.7%. The remaining tracer, not recovered by sampling, probably moved outside the 5 cm strip above the needles by diffusion and dispersion. A numerical simulation was performed with Hydrus2D to check the plume aspect and the coherence of the results, taking in account that the paint coating sealed one side of the soil column (Fig. 4). A steady state of water flux was assumed, and the soil water flow parameters used in the simulation were those measured at the 53-cm depth (Table 1). The soil water content profile was set to correspond to the values from Fig. 2 for the van Genuchten soil parameters set at a depth of 53 cm. According to the lower convective speed measured with the tracer, K_s was set to 375 cm d^{-1} to coincide with the maximum of contents (0.22 cm min^{-1}). The best fit with inverse modeling was then computed for isotopic contents and was found for longitudinal and lateral dispersion of 8.15 cm and 2.24 cm, respectively (Fig. 4). The tracer recovery rate based on this run was computed to be 48.5%, and this agrees well with the estimate based on measurements.

4 Discussion

The water flow values computed using soil characteristics determined at the laboratory were systematically higher than the capillary rise flux found from tracer displacement. The latter is dependent on the evaluations of the peak displacement and the average water content of the soil between the injection point and the peak. If the uncertainties on tracer displacement and water content were ±0.5 cm and ±1% respectively, then the evaporation flux would be between 2.7 cm y^{-1} and 4.4 cm y^{-1}; therefore, lower values cannot easily be attributed to measurement error. Considering a soil volume of 1 cm^3 with a water content of 7%, the increased water content due to the injection of the tracer solution (6 µL) represented less than 10% relative to the initial content. Consequently, the perturbation of the water regime by the injection should be negligible, thus justifying the use of high ^{2}H concentration in the injected solution. The steady state of the evaporation rate was a main assumption used to compute fluxes via integration of the unsaturated hydraulic conductivity and tension head functions. To check that equilibrium was reached during the experiment, we used Hydrus 1-D and simulated the evolution of the soil profile from 0.5 m to 2.44 m from the beginning of the year, for all the sets of laboratory hydrodynamic parameters. The upper boundary conditions were representative, in the upper cell, of the daily precipitation records from the nearest meteorological station and the evaporation demand was fixed to 0.5 cm d^{-1}. The maximum suction of the upper cell was set to the potential head, corresponding to a water content of 0.0495 (Table 2). The lower boundary condition was soil water saturation at the 2.44-m depth. Although the initial condition assumed the water saturation of the profile, all simulations indicated a steady-state evaporation regime between the injection and sampling dates, and the water regime was stabilized in less than 50 days (Fig. 5). Consequently, it can be assumed that

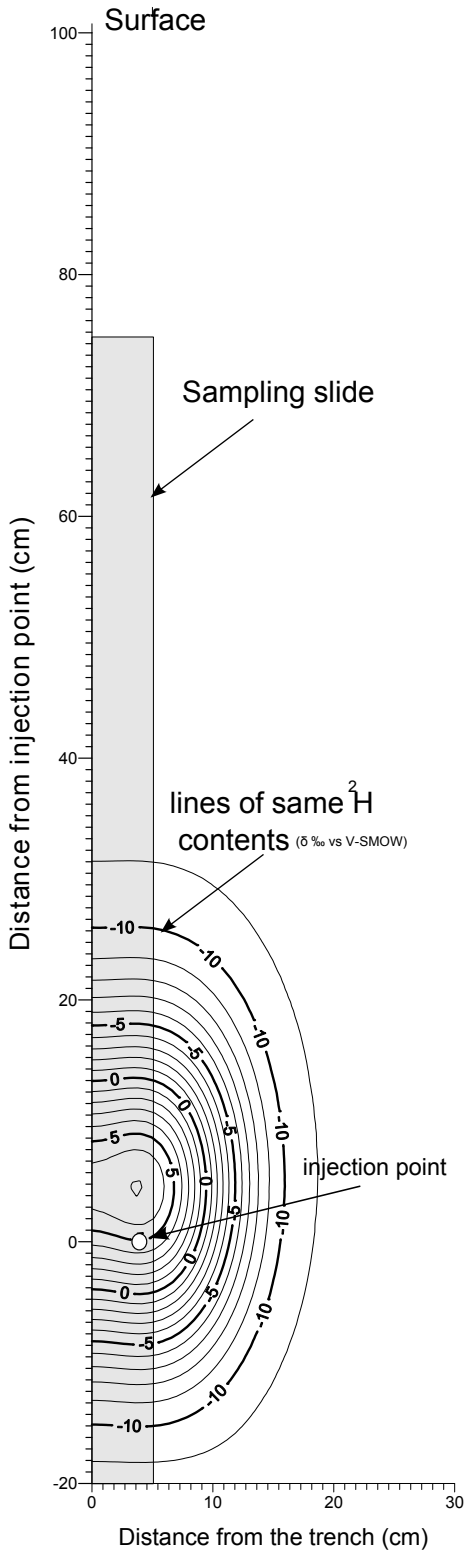

Fig. 4. Isocurves of ^{2}H contents (δ ‰ vs. V-SMOW) after 35 days of tracer displacement simulated with Hydrus 2D. $\Theta_r = 0.0304$, Θ_S, $= 0.287$, $\alpha = 0.0304\,cm^{-1}$, $K_s = 0.22$ cm min^{-1}, $n = 2.207$. Longitudinal dispersivity = 8.15 cm, Lateral dispersivity = 2.24 cm assuming a water regime at steady state between injection and recovering.

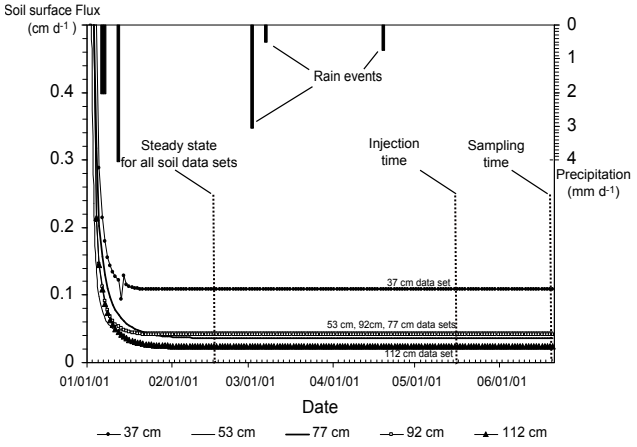

Fig. 5. Simulation of the steady-state establishment for five different van Genuchten soil parameters sets, assuming an initial saturation of soil profile from 0.50 m to 2.44 m depths at the beginning of the year 2001. Uprising fluxes computed with Hydrus 1D (right axis, cm d^{-1}) and rain events (left axis, mm d^{-1}). Boundary conditions reflecting: (i) meteorological data (rain events and potential evaporation of 5 mm d^{-1} and maximum suction head corresponding to 0.0495 water content at the upper cell (0.5 m depth), (ii) Lower boundary condition fixed with water saturation at 2.44 m depth. The top layer (0 to 0.5 m depth) was not considered in the simulation.

a discrepancy from the steady-state water regime was not the reason for the over estimation of fluxes. A cumulative flow of 0.351 cm between the injection and sampling dates was consistent with the observation of a constant aquifer level depth during this period, i.e., the cumulative flux would be related to a 1 cm increase in saturation depth, which is roughly the accuracy of the piezometric measurement. Steady-state rates higher than the value computed from the peak displacement cannot be explained by a rising of the water-table level or by lower water contents, which would emphasize the difference. The effect of lowering the water-table level by 10 cm (making it 2.54 m instead of 2.44 m) would not be enough to account for the observed difference; however, the steady-state fluxes obtained for 35 days by setting the upper boundary condition to higher water content (0.0595 at 50 cm) would define a large range [0.14 to 3.27 cm] (Table 4). This wide value range includes the value computed from the peak displacement (0.351 cm for 35 days).

Gowing et al. (2005) emphasized the influence of vapor–liquid phase transition occurring in the upper parts of the profile on the evaporation flux. Measurements of relative humidity performed from the soil surface to a depth of 31 cm revealed that during the study period, evaporation front was presumably located above a depth of 40 cm; at this depth, pore air moisture was saturated with water vapor even during the mid-day maximum drought. Indeed, at depths greater than 31 cm (Table 1), relative humidity was always higher than 80%, and at depth of 50 cm, the potential head computed from the measured water contents (1) and Eq. (2) lead

to a maximum suction of −455.3 cm (Table 2). These ranges of potential head and moisture are clearly characteristic of dominant liquid transfer. Near steady state, in the top layer of a dry soil, the evaporation front depth was related to the inverse of the evaporation rate (Barnes et Allison, 1983). For instance, under similar conditions in a sandy loam in Northeast Thailand at the end of the dry season, Grunberger et al. (2008) found the evaporation front to be located at a depth of 12 cm for a rate of evaporation of 82 mm y^{-1}. Considering the range of evaporation rates measured in the present study (36 mm y^{-1}), the depth of the evaporation front would be established at around 27 cm depth. Inside the water vapor transfer layer (VTL), processes are not well represented by the equations developed inside the van Genuchten formalism. Moreover, tension head values higher than −800 cm are not easily measured, thus impeding correct extrapolations in very dry soil. Hence, resolution of the Richard equation based on the extrapolation of the relationships defining hydraulic conductivity, tension heads and water contents is questionable. This would explain the over-estimations encountered when the integration function is applied to high suctions. For soil layers deeper than 50 cm, the water content values correspond to tension heads falling within the range of the tension heads that were measured in the laboratory (> −800 cm). Inside VTL, vapor flow processes may drive the evaporation flux, but quantifications based on water contents measured under the VTL should correspond to the same rate if a steady state of evaporation is assumed. No hydrodynamic characteristics were determined for soil layers at less than 1 m depth because lower excavation would have endangered the stability of the floor of the pit, due to increasing water content near the aquifer water level. However, deeper soil layers could present lower permeability, particularly when close to the permanent water saturation level, at which point pedogenesis processes may favor clay formation. In the case of deep layers with lower hydraulic conductivity values, discrepancies should be observed between estimates (*i*) and (*ii*) based on extrapolations of soil characteristics to 2.44 m depth and estimate (*iii*), based on 37 cm to 100 cm depths (Table 2). The assumption could not be sustained because no strong differences of fluxes were observed in this study. Based on the compilation of 20 different isotopic profiles Coudrain-Ribstein et al. (1998) proposed a relationship linking depth and evaporation flux that would imply a rate of 1.9 cm y^{-1} for the observed aquifer depth (2.44 m). Our measured rate is 1.8-times higher than this value. Nevertheless, the experimental value (3.7 cm y^{-1}) is included in the range defined by the same authors after making high suction permeability measurements on loamy and sandy soils [6 mm y^{-1} to 49 mm y^{-1}].

5 Conclusions

Field tracer (deuterium) introduction in the wall of a soil pit and sampling after 35 days showed a peak displacement that could be interpreted as the result of a slow water rise from the aquifer. This study provided an alternative method for the estimation of water flux in soils to previous methods based on natural isotopic contents and/or measuring soil hydrodynamic features. Compared to other methods, the presented method has the following assumptions: (i) the "peak displacement method" is not based on the stability of water regime in the soil between injection and sampling times and therefore does not require any steady-state assumption. A strong limitation rises from the need to retrieve the tracer peak from the soil, and thus previous knowledge of the expected range of displacement is necessary; (ii) in addition to isotope data, only data about density and water contents in the zone of the tracer peak are necessary; (iii) the measurement is cumulative over a predetermined period, which avoids the need for considerations of night and day alternation and particular sampling times; (iv) the method does not require any knowledge of soil characteristics below and above the sampling zone, but the assimilation of peak displacement to the evaporation flux through the profile requires a steady-state assumption. In the case of the studied experimental site, a value of 3.7 cm y^{-1} was proposed. This value is higher than other estimates based on natural diffusion of water isotopes with the same aquifer depths (Coudrain et al., 1998). However, it is lower than all the estimates based on the laboratory soil determination of the van Genuchten closed-form functions for soil hydraulic conductivity and retention curve, either using an integration procedure or a Hydrus profile simulation with realistic boundary conditions.

Appendix A

List of parameters

E	Convective flux (cm d^{-1}) or (mm y^{-1})
$E_{35\ \mathrm{days}}$	Cumulative convective flux during 35 days (cm)
z, inj, peak Depth (cm),	Injection depth (cm), Peak of isotopic content depth (cm)
$\psi, \psi\ (z), \psi$	i Tension heads (cm), at depth z, at step i
ψ_1, ψ_2	Integration limits for tension heads: tension 1 (cm), tension 2 (cm)
$\Theta, \Theta(z), \Theta_r, \Theta_s$	Volumetric water content, at depth z, residual, saturated ($cm^3\ cm^{-3}$)
S, $S(\theta)$, $S(\psi)$	Saturation index, at water content Θ, at tension head Ψ

K, K_s, $K(\psi)$	Hydraulic conductivity, at saturation, at tension head Ψ ($cm\,d^{-1}$)
α	van Genuchten parameter (cm^{-1})
n, m	van Genuchten parameters ($m = 1-1/n$)
z_1, z_2	Integration limits depths: depth 1 (cm), depth 2 (cm)
$\Delta\psi i$	Integration step (cm) for potential head at step i
λ, γ	Value of integration steps: proportional step, constant step (cm)

Acknowledgements. Authors are grateful for the help provided by: (i) Dindnane Khalid, Student of Agadir University who helped us during the injection and sampling field operation, including a 24 h monitoring of soil and air humidity. (ii) Jean Larvy De Larivière, IRD technical staff who realized all soil characterization procedures. (iii) Annick Filly, Université Paris-Sud, who supervised isotopic determinations. iv) Pascal Boivin, former head of IRD research unit ARIANE (1999–2004) who encouraged us allocating field operational costs of the unit to this research action.

Edited by: T. P. A. Ferre

References

Allison, G. B.: The relationship between 18O and Deuterium in water and sand columns undergoing evaporation, J. Hydrol., 55, 163–169, 1982.

Barnes, C. J. and Allison, G. B. : The distribution of deuterium and 18O in dry soils 1. Theory, J. Hydrol., 60, 141–156, 1983.

Barnes, C. J. and Allison, G. B.,: The distribution of deuterium and 18O in dry soils.3-Theory for non isothermal water movement, J. Hydrol., 74, 119–135, 1984.

Barnes, C. J. and Allison, G. B.: Tracing of water movement in the unsatured zone using stable isotopes of hydrogen and oxygen, J. Hydrol. 100, 143–176, 1988.

Barnes, C. J. and Hughes, M. W.: The use of natural tracers as indicators of soil water movement in a temperate semi arid region, J. Hydrol., 60, 157–173, 1983.

Barnes, C. J. and Walker, G. B.: The distribution of deuterium and Oxygen 18 during unsteady evaporation, J. Hydrol., 112, 55–67, 1989.

Bouchaou, L., Michelot, J. L., Vengosh, A., Hsissou, Y., Qurtobi, M., Gaye, C. B., Bullen, T. D., and Zuppi, G. M.: Application of multiple isotopic and geochemical tracers for investigation of recharge, salinization, and residence time of water in the Souss–Massa aquifer, southwest of Morocco, J. Hydrol., 352, 267–287, 2008

Braud, I., Bariac, T., Gaudet, J. P., and Vauclin, M.: SiSPAT-Isotope, a coupled heat, water and stable isotope (HDO and $H_2^{18}O$) transport model for bare soil. Part I. Model description and first verifications, J. of Hydrol., 309, 277–300, 2005a.

Braud, I., Bariac, T., Vauclin, M., Boujamlaoui, Z., Gaudet, J. P., Biron, Ph., and Richard, P.: SiSPAT-Isotope, a coupled heat, water and stable isotope (HDO and $H_2^{18}O$) transport model for bare soil. Part II. Evaluation and sensitivity tests using two laboratory data sets, J. Hydrol., 309, 301–320, 2005b.

Brunel, J. P., Walker, G. R., and Kennet-Smith, A. K.: Field validation of isotopic procedures for determining sources of water used by plants in a semi-arid environment, J. Hydrol. 167, 351–368, 1995.

Brunel, J. P., Walker, G. R., Dighton, J. C., and Monteny, B.: Use of stable isotopes of water to determine the origin of water used by the vegetation and to partition of evapotranspiration a case of study from Hapex-Sahel, J. Hydrol., 188, 466–481, 1997.

Coleman, M. L., Shepherd, T. J., Durham, J. J., Rouse, J. E., and Moore, G. R.: Reduction of Water with Zinc for Hydrogen Isotope Analysis, Anal. Chem., 54, 993–995, 1982.

Coudrain-Ribstein, A., Pratx, B., Talbi, A., and Jusserand, C.: Is the evaporation from phreatic aquifers in arid zones independent of the soil characteristics?, C. R. Acad. Sci., Ser. II., Sci. Terr. Plan., 326, 159–165, 1998.

Fontes, J. C., Yousfi, M., and Allison, G. B. : Estimation of the long term diffuse groundwater discharge in the northern Sahara using stable isotope profiles of soil water, J. Hydrol., 86, 315–327, 1986.

Garcia, C. A., Andraski, B. J., Stonestrom, D. A., Cooper, C. A., Johnson, M. J., Michel, R. L., and Wheatcraft, S. W.: Transport of Tritium Contamination to the Atmosphere in an Arid Environment, Vadose Zone J., 8, 450-461, 2009

Gardner, W. R.: Some steady state solutions of the unsaturated moisture flow equation with application to evaporation from water table, Soil Sci., 85(4), 228–232, 1958.

Gardner, W. R. and Fireman, M.: Laboratory studies of evaporation from soil columns in the presence of a water table. Soil Science. 84(5), 244–249, 1958.

Garcia, C. A., Andraski, B. J., Stonestrom, D. A., Cooper C. A., Johnson, M. J., Michel, R. L., and Wheatcraft, S. W.: Transport of Tritium Contamination to the Atmosphere in an Arid Environment, Vadose Zone J. 2009. 8:450-461,2009

Grünberger, O., Macaigne, P., Michelot, J. L., Hartmann, C., and Sukchan, S.: Salt crust development in paddy fields owing to soil evaporation and drainage: Contribution of chloride and deuterium profile analysis, J. Hydrol., 348, 110–123, 2008.

Gowing, J. W. F., Konukcu, F., and Rose, D. A.: Evaporative flux from a shallow water table: The influence of a vapour–liquid phase transition, J. Hydrol., 321, 77–89, 2008.

Jim Yeh, T.-C. and Harvey, D. J.: Effective unsaturated hydraulic conductivity of layered sands, Water Resour. Res., 26(6), 1271–1279, 1990.

Hu, S. J. , Lei, J. Q., Xu, X. W., Song, Y. D., Tian, C. Y., Chen, X. B., Li, X. C.: Theoretical analysis of the limiting rate of phreatic evaporation for aeolian sandy soil in Taklimakan Desert, Chinese Sci. Bull., 53, 119–124, 2008.

Koeniger, P., Leibundgut C., Link, T., and Marshall, J. D.: Stable isotopes applied as water tracers in column and field studies, Org. Geochem., 41, 31–40, 2010.

Liu, B., Phillips, F., Hoines, S., Campbell, A. R., and Sharma, P.: Water movement in desert soil traced by hydrogen and oxygen isotopes, chloride, and chlorine-36, southern Arizona, J. Hydrol., 168, 91–110, 1995.

Marc, V. and Robinson, M.: Application of the deuterium tracing method for the estimation of tree sap flow and stand transpiration of a beech forest (Fagus silvatica L.) in a mountainous Mediter-

ranean region, J. Hydrol., 285, 248–259, 2004.
Melayah, L. and Bruckler, L.: Modeling the transport of water stable isotopes in unsatured soils under natural conditions. 1 Theory, Water Resour. Res., 32(7), 2047–2054, 1996a.
Melayah, L. and Bruckler, L.: Modeling the transport of water stable isotopes in unsatured soils under natural conditions. 2. Comparison with field experiment, Water Resourc. Res. 32(7), 2055–2065, 1996b.
Simunek, J., Wendroth, O., and Van Genuchten, M. Th.: Parameter Estimation Analysis of the Evaporation Method for Determining Soil Hydraulic Properties, Soil. Sci. Soc. Am. J., 62, 894–905, 1998.
Shimojima, E., Curtis Alan, A., and Turner Jeffrey, V.: The mechanism of evaporation from sand columns with restricted and unrestricted water tables using deuterium under turbulent airflow conditions, J. Hydrol., 117, 15–54, 1990.
Stour, L., Agoumi, A.: Climatic drought in Morocco during the last decades, Hydroécol. Appl., 16, 215–232, 2008.
Van Genuchten, M. Th.: A closed-form equation for predicting the hydraulic conductivity of unsaturated soils, Soil Sci. Soc. Am. J., 44, 892–898, 1980.
Yamanaka, T. and Yonetani, T.: Dynamics of the evaporation zone in dry sandy soils, J. Hydrol., 217, 135–148. 1999.
Walker, C. D. and Brunel, J. P.: Examining evapotranspriration in a semi arid region using stable isotopes of hydrogen and oxygen. J. Hydrol., 118, 55–75, 1990.
Walker, C. D., Hughes, M. W., Allison, G. B., and Barnes, C. J.: The movement of isotopes of water during evaporation from a bare soil surface, J. Hydrol., 181, 181–197. 1988.
Weisrock, A. Adèle, B. and Tannouch-Bennani, S. Dunes littorales et dunes continentales au Maroc atlantique semi-aride (29–30 N) du Pléistocène supérieur à l'actuel, Revista C&G, 16(1–4), 43–56, 2002.
Wind, G. P.: Capillary conductivity data estimated by a simple method, In Proc. Wageningen Symp., June 1966, 1, 181–191, IASAH, Gentbrugge, Belgium, 1968.